

We are IntechOpen, the world's leading publisher of Open Access books Built by scientists, for scientists

6,900

Open access books available

185,000

International authors and editors

200M

Downloads

Our authors are among the

154

Countries delivered to

TOP 1%

most cited scientists

12.2%

Contributors from top 500 universities



WEB OF SCIENCE™

Selection of our books indexed in the Book Citation Index
in Web of Science™ Core Collection (BKCI)

Interested in publishing with us?
Contact book.department@intechopen.com

Numbers displayed above are based on latest data collected.
For more information visit www.intechopen.com



New Variants to Theoretical Investigations of Thermosyphon Loop

Henryk Bieliński

*The Szewalski Institute of Fluid-Flow Machinery, Polish Academy of Sciences, Gdańsk
Poland*

1. Introduction

The purpose of this chapter is to present three variants of the generalized model of thermosyphon loop, using a detailed analysis of heat transfer and fluid flow (Bieliński & Mikieliewicz, 2011). This theoretical investigation of thermosyphon loop is based on analytical and numerical calculations. The first variant of thermosyphon loop (HHVCHV) is composed of two heated sides: the lower horizontal and vertical sides and two cooled sides: the upper horizontal and vertical opposite sides. This variant is made for conventional tubes and has a one-phase fluid as the working substance. The second variant of thermosyphon loop (2H2C) is consisted of two lower evaporators: horizontal and vertical and two upper condensers: horizontal and vertical and is made for minichannels. The third variant of thermosyphon loop has an evaporator on the lower horizontal section and a condenser on the upper vertical section. This variant contains minichannels and a supporting minipump (HHCV+P). A two-phase fluid is used as the working substance in the second and third variants.

The new variants reported in the present study is a continuation and an extension of earlier work *"Natural Circulation in Single and Two Phase Thermosyphon Loop with Conventional Tubes and Minichannels."* published by InTech (ISBN 978-953-307-550-1) in book *"Heat Transfer. Mathematical Modelling, Numerical Methods and Information Technology"*, Edited by A. Belmiloudi, pp. 475-496, (2011). This previous work starts a discussion of the generalized model for the thermosyphon loop and describes three variants. In the first variant (HHCH) the lower horizontal side of the thermosyphon loop was heated and its upper horizontal side was cooled. In the second variant (HVCV) the lower part of vertical side of the thermosyphon loop was heated and its upper part at opposite vertical side was cooled. In the third variant (HHCV) a section of the lower horizontal side of the thermosyphon loop was heated and its upper section of vertical side was cooled. A one- and two-phase fluid were used as a working substance in the first and in both second and third variants of the thermosyphon loop, respectively. Additionally, the first variant was made for conventional tubes and the second and third variants were made for minichannels. It was necessary in case of the thermosyphon loop with minichannels to apply some new correlations for the void fraction and the local two-phase friction coefficient in both two-phase regions: adiabatic and diabatic, and the local heat transfer coefficient in flow boiling and condensation. Some other variants to theoretical investigations of the generalized model for thermosyphon loop are demonstrated in (Bieliński & Mikieliewicz, 2004, 2005, 2010).

Fluid flow of thermosyphon loop is created by the buoyancy forces that evolve from the density gradients induced by temperature differences in the heating and cooling sections of the loop. An advanced thermosyphon loop is composed of an evaporator and a condenser; a riser and a downcomer connect these parts. A liquid boils into its vapour phase in the evaporator and the vapour condenses back to a liquid in the condenser. The thermosyphon loop is a simple passive heat transfer device, which relies on gravity for returning the liquid to the evaporator. The thermosyphon loops are a far better solution than other cooling systems because they are pumpless. In such cases, when mass flow rate is not high enough to circulate the necessary fluid to transport heat from evaporator to condenser, the use of a pump is necessary. The presented study considers the case where the buoyancy term and the pump term in the momentum equation are of the same order.

The following applications for thermosyphon loops are well-known, such as solar water heaters, thermosyphon reboilers, geothermal systems, emergency cooling systems in nuclear reactor cores, thermal diodes and electronic device cooling. The thermal diode is based on natural circulation of the fluid around the closed-loop thermosyphon (Bieliński & Mikielewicz, 1995, 2001), (Chen, 1998). The closed-loop thermosyphon is also known as a “liquid fin” (Madejski & Mikielewicz, 1971).

Numerous investigations, both theoretical and experimental have been conducted to study of the fluid behaviour in thermosyphon loops. Zvirin (Zvirin, 1981) presented results of theoretical and experimental studies concerned with natural circulation loops, and modelling methods describing steady state flows, transient and stability characteristics. Ramos (Ramos et al., 1985) performed the theoretical study of the steady state flow in the two-phase thermosyphon loop with conventional tube. Greif (Greif, 1988) reviewed basic experimental and theoretical work on natural circulation loops. Vijayan (Vijayan et al., 2005) compared the dynamic behaviour of the single- and two-phase thermosyphon loop with conventional tube and the different displacement of heater and cooler. Misale (Misale et al., 2007) reports an experimental investigations related to rectangular single-phase natural circulation mini-loop.

The present study provides in-depth analysis of heat transfer and fluid flow using three new variants of the generalized model of thermosyphon loop. Each individual variant can be analyzed in terms of single- and two-phase flow in the thermosyphon loop with conventional tubes and minichannels. In order to analyse the numerical results of simulation for the two-phase flow and heat transfer in the thermosyphon loop, the empirical correlations for the heat transfer coefficient in flow boiling and condensation, and two-phase friction factor in diabatic and adiabatic sectors in minichannels, are used. The analysis of the thermosyphon loop is based on the one-dimensional model, which includes mass, momentum and energy balances. The separate two-phase flow model is used in calculations. A numerical investigation for the analysis of the mass flux and heat transfer coefficient in the steady state has been done. The effect of thermal and geometrical parameters of the loop on the mass flux in the steady state is examined numerically.

The El-Hajal correlation for void fraction (El-Hajal et al., 2003), the Zhang-Webb correlation for the friction pressure drop of two-phase flow in adiabatic region (Zhang & Webb, 2001), the Tran correlation for the friction pressure drop of two-phase flow in diabatic region (Tran et al. 2000), the Mikielewicz (Mikielewicz et al., 2007) and the Saitoh (Saitoh et al., 2007) correlations for the flow boiling heat transfer coefficient in minichannels, the Mikielewicz (Mikielewicz et al., 2007) and the Tang (Tang et al., 2000) correlations for condensation heat transfer coefficient in minichannels has been used to evaluate the thermosyphon loop with minichannels.

Finally, theoretical investigations of the variants associated with the generalized model of thermosyphon loop can offer practical advice for technical and research purposes.

2. Single phase thermosyphon loop heated from lower horizontal and vertical side and cooled from upper horizontal and vertical side

This single-phase variant of thermosyphon loop is heated from below horizontal section ($s_0 \leq s \leq s_1$) and vertical section ($s_1 \leq s \leq s_2$) by a constant heat flux: \dot{q}_H . Constant heat flux \dot{q}_H spaced in cross-section area per heated length: L_H . In the upper horizontal section ($s_3 \leq s \leq s_4$) and opposite vertical section ($s_4 \leq s \leq s_5$) the thermosyphon loop gives heat to the environment. The heat transfer coefficient between the wall and environment, α_c , and the temperature of the environment, T_0 , are assumed constant. The heated and cooled parts of the thermosyphon loop are connected by perfectly isolated channels ($s_2 \leq s \leq s_3$; $s_5 \leq s \leq s_6$).

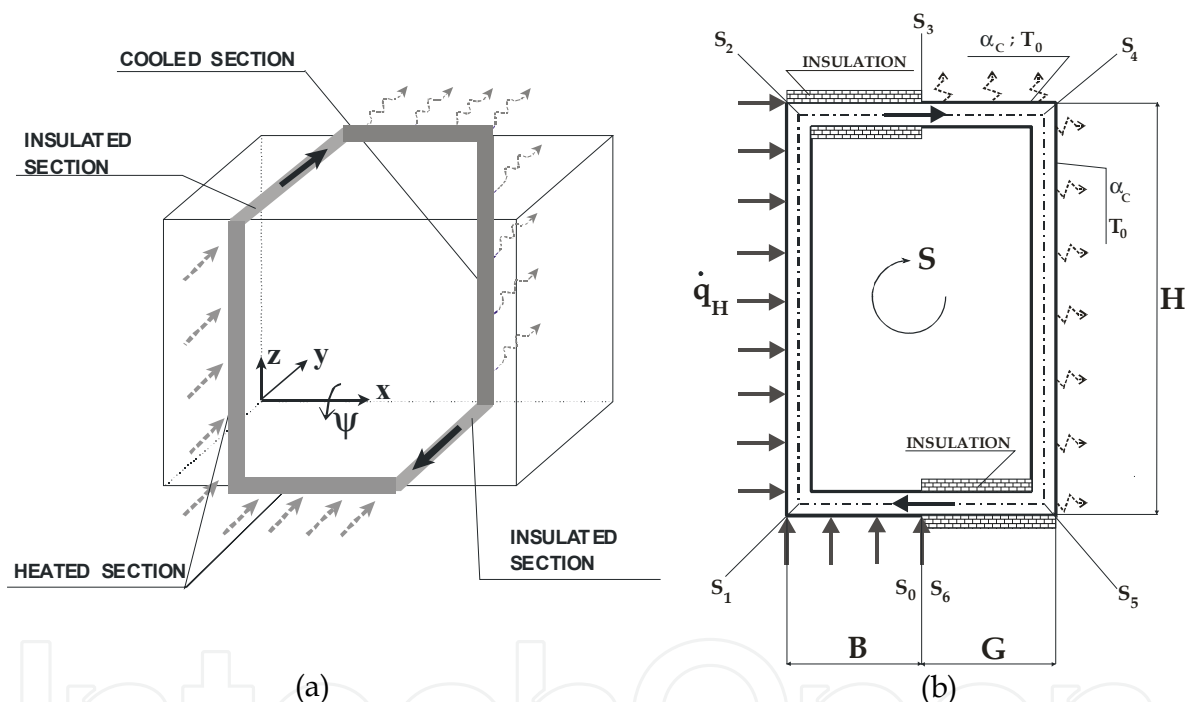


Fig. 1. The variant of single phase thermosyphon loop heated from lower horizontal and vertical side and cooled from upper horizontal and opposite vertical side (HHVCHV). (a) 3Dimensional, (b) 2D

The space co-ordinate s circulates around the closed loop as shown in Fig. 1(b). The total length of the loop is denoted by L , cross-section area of the channel is A , wetted perimeter is U . Thermal properties of fluid: ρ - density, c_p - heat capacity of constant pressure, λ - thermal conductivity.

The following assumptions are used in the theoretical model of natural circulation in the closed loop thermosyphon:

1. thermal equilibrium exists at any point of the loop,
2. incompressibility, because the flow velocity in the natural circulation loop is relatively low compared with the acoustic speed of the fluid under current model conditions,

3. viscous dissipation in fluid is neglected in the energy equations,
4. heat losses in the thermosyphon loop are negligible,
5. $(D/L) \ll 1$; one-dimensional models are used and the flow is fully mixed. The velocity and temperature variation at any cross section is therefore neglected. The flow is fully developed and the temperature is uniform at the steady state,
6. single-phase fluid can be selected as the working fluid,
7. curvature effects and associated form losses are negligible,
8. fluid properties are constants, except density in the gravity term. The Boussinsq approximation is valid for a single-phase system, then density is assumed to vary as $\rho = \rho_0 \cdot [1 - \beta \cdot (T - T_0)]$ in the gravity term where $\beta = \frac{1}{v_0} \cdot \left(\frac{\partial v}{\partial T} \right)_p$ (v - specific volume, "0" is the reference of steady state),
9. the effect of superheating and subcooling are neglected.

Under the above assumptions, the governing equations for natural circulation systems can be written as follows:

- conservation of mass:

$$\frac{\partial \rho}{\partial \tau} + \frac{\partial}{\partial s}(\rho \cdot w) = 0 \quad ; \quad (1)$$

where τ - time, w - velocity.

- conservation of momentum:

$$\rho \cdot \left(\frac{\partial w}{\partial \tau} + w \cdot \frac{\partial w}{\partial s} \right) = - \frac{\partial p}{\partial s} + \varepsilon \cdot \rho \cdot \tilde{g} - \tau_w \cdot \frac{U}{A} \quad ; \quad (2)$$

where $\varepsilon = 0$ for $\vec{e} \perp \vec{g}$; $\varepsilon = (+1)$ for $\vec{e} \uparrow \wedge \vec{g} \downarrow$; $\varepsilon = (-1)$ for $\vec{e} \downarrow \wedge \vec{g} \downarrow$; $\tilde{g} = \vec{e} \circ \vec{g} = 1 \cdot g \cdot \cos(\vec{e}, \vec{g})$; $|\vec{g}| = g$; $|\vec{e}| = 1$; \vec{e} is a versor of the coordinate around the loop, and τ_w - wall shear stress.

- conservation of energy:

$$\frac{\partial T}{\partial \tau} + w \cdot \frac{\partial T}{\partial s} = a_0 \cdot \frac{\partial^2 T}{\partial s^2} \begin{cases} + 0 & \text{for adiabatic section} \\ - \frac{q_c \cdot U_c}{c_{p0} \cdot \rho_0 \cdot A} & \text{for cooled section} \\ + \frac{\dot{q}_H \cdot U_H}{c_{p0} \cdot \rho_0 \cdot A} & \text{for heated section} \end{cases} \quad (3)$$

where $a_0 = \frac{\lambda_0}{\rho_0 \cdot c_{p0}}$ - thermal diffusivity,

In order to eliminate the pressure gradient and the acceleration term, the momentum equation in Eq. (2) is integrated around the loop $\oint \left(\frac{\partial p}{\partial s} \right) ds = 0$.

The flow in natural circulation systems which is driven by density distribution is also known as a gravity driven flow or thermosyphonic flow. The momentum and the energy equations in such flows are coupled and for this reason they must be solved simultaneously (Mikielewicz, 1995).

The above governing equations can be transformed to their dimensionless forms by the following scaling:

$$\tau^+ = (a_0 \cdot \tau) / L^2 ; \quad s^+ = s / L ; \quad \dot{m}^+ = (\dot{m} \cdot L) / (a_0 \cdot \rho_0 \cdot A) ; \quad T^+ = \frac{\lambda_0 \cdot (A / U_H) \cdot (T - T_0)}{(\dot{q}_H \cdot L^2)} ; \quad (4)$$

The dimensionless momentum equation and the energy equation at the steady state for the thermosyphon loop heated from below can be written as follows:

- momentum equation (with: $K_j = s_j / L$;) and $\theta = \begin{cases} 1 & \text{for laminar flow} \\ 7/4 & \text{for turbulent flow} \end{cases}$;

$$(\dot{m}^+)^{\theta} = (Ra)^{**} (-1) \cdot \left[\int_0^1 T^+ \cdot \cos(\vec{e}, \vec{g}) \, ds^+ \right] ; \quad (5)$$

- energy equation

$$\dot{m}^+ \frac{dT^+}{ds^+} = \frac{d^2 T^+}{ds^{+2}} \begin{cases} +0 & \text{insulated sections} \\ -(Bi)^{**} \cdot T^+ & \text{for cooling section} \\ +1 & \text{heater section} \end{cases} \quad (6)$$

with boundary conditions

$$\begin{aligned} T_{A1}^+(K_2) &= T_H^+(K_2) ; \quad T_{A1}^+(K_3) = T_C^+(K_3) ; \quad T_C^+(K_5) = T_{A2}^+(K_5) ; \quad T_{A2}^+(1) = T_H^+(0) ; \\ \frac{dT_{A1}^+}{ds^+} \Big|_{s^+=K_2} &= \frac{dT_H^+}{ds^+} \Big|_{s^+=K_2} ; \quad \frac{dT_{A1}^+}{ds^+} \Big|_{s^+=K_3} = \frac{dT_C^+}{ds^+} \Big|_{s^+=K_3} ; \\ \frac{dT_C^+}{ds^+} \Big|_{s^+=K_5} &= \frac{dT_{A2}^+}{ds^+} \Big|_{s^+=K_5} ; \quad \frac{dT_{A2}^+}{ds^+} \Big|_{s^+=1} = \frac{dT_H^+}{ds^+} \Big|_{s^+=0} ; \end{aligned} \quad (7)$$

The parameters appearing in the momentum and the energy equations are the modified Biot, Rayleigh and Prandtl numbers.

$$(Bi)^{**} = \frac{\alpha_c \cdot U_c \cdot L^2}{\lambda_0 \cdot A} ; \quad (8)$$

for laminar flow: ($\theta = 1$)

$$(Ra)_l^{**} = \frac{g \cdot \beta_0 \cdot L^3 \cdot (\dot{q}_H / \lambda_0)}{v_0 \cdot a_0} \cdot \frac{A \cdot U_H}{2 \cdot U^2} ; \quad (Pr)_l^{**} = 2 \cdot L^2 \cdot \left(\frac{U}{A} \right)^2 \cdot \left(\frac{v_0}{a_0} \right) ; \quad (9)$$

for turbulent flow: $(\theta = 7/4)$

$$(Ra)_t^{**} = \frac{\sqrt{128}}{0.3164} \cdot \frac{g \cdot \beta_0 \cdot (L)^{15/4} \cdot (\dot{q}_H / \lambda_0)}{(v_0)^{1/4} \cdot (a_0)^{7/4}} \cdot \frac{(A)^{1/4} \cdot U_H}{(U)^{5/4}}; \quad (Pr)_t^{**} = \frac{0.3164}{\sqrt{128}} \cdot \left(\frac{L \cdot U}{A} \right)^{5/4} \cdot \left(\frac{v_0}{a_0} \right)^{1/4}; \quad (10)$$

In the case of the laminar and turbulent steady-state flow, the dimensionless distributions of temperature around the loop can be obtained analytically from Eq. (6). The distilled water was used as the working fluid. It has been found that the Biot number has an influence on temperature in the laminar and turbulent flow. The results are shown in Figs. 2 and 3.

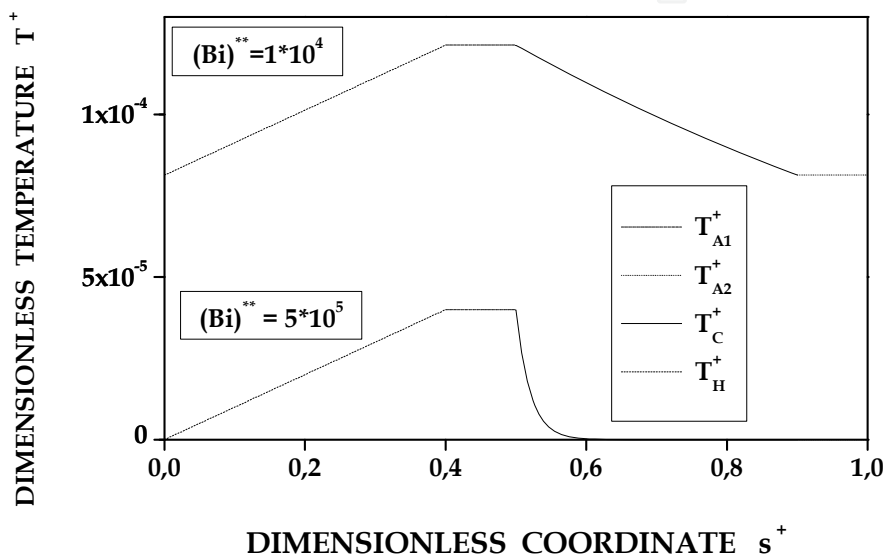


Fig. 2. The effect of Biot number on temperatures in the laminar steady-state flow (HHVCHV)

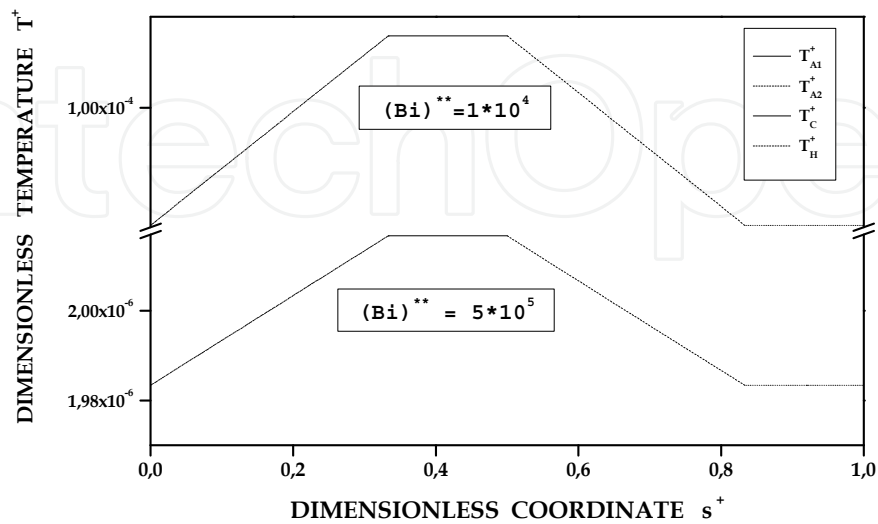


Fig. 3. The effect of Biot number on temperatures in the turbulent steady-state flow (HHVCHV)

The effect of the loop’s aspect ratio (breadth B to height H) on the mass flow rate found numerically in the case of laminar flow at the steady state is presented in Fig. 4 .

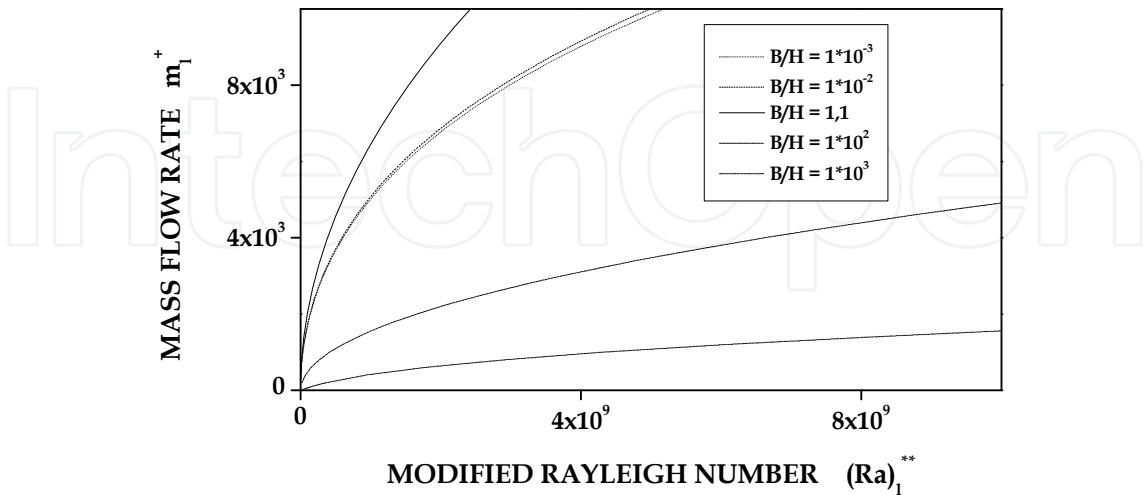


Fig. 4. Mass flow rate for laminar flow at the steady state versus modified Rayleigh number at different B/H ratios (HHVCHV)

For this variant of the thermosyphon loop it has been found that the maximum of the mass flow rate appears for $B/H=1,1$.
The effect of geometrical parameter of the loop (length of insulation section G to height H) on the mass flow rate found numerically in the case of laminar flow at the steady state is presented in Fig. 5. The mass flow rate increases with decreasing G/H aspect ratio, due to the decreasing frictional pressure term.

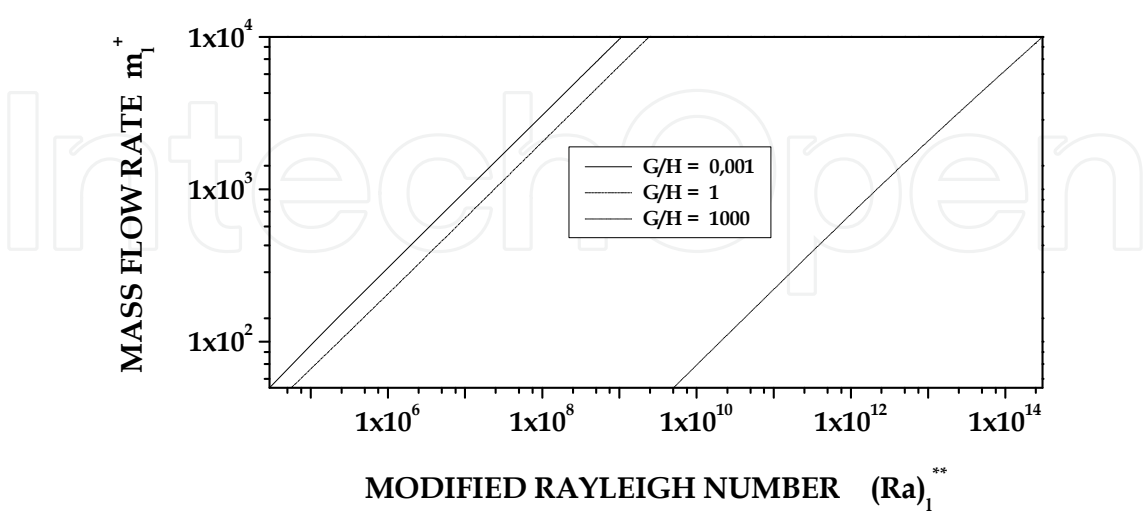


Fig. 5. Mass flow rate for laminar flow at the steady state versus modified Rayleigh number at different G/H ratios (HHVCHV)

This paper presents the case of the onset of motion of the single-phase fluid from a rest state if the loop rotates 90 degrees around the x-axis. The heated sections can be presented in the horizontal plane below the cooled sections. The presented numerical calculations are based on a new method for solution of the problem for the onset of motion in the fluid from the rest (Bieliński & Mikielwicz, 2005). Conditions for the onset of motion in the thermosyphon can be determined by considering the steady solutions with circulation for the limiting case of $\dot{m}_1^+ \rightarrow 0$.

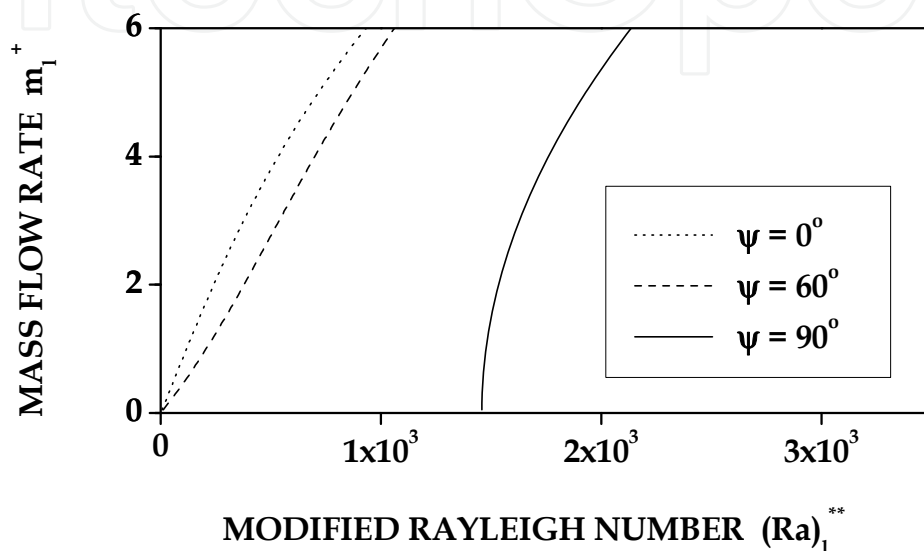


Fig. 6. The case of the onset of motion of the single-phase fluid from a rest state if the loop rotates 90 degrees around the x-axis (HHVCHV+ $\psi 90^\circ$)

The analysis was based on the equations of motion and energy for the steady-state conditions. The heat conduction term has to be taken into account in this approach because the heat transfer due to conduction is becoming an increasingly important factor for decreasing mass flow rates. The fluid starts circulation around the loop, when the Rayleigh number exceeds a critical value, which can be found using the method $\dot{m}_1^+ \rightarrow 0$ for the $\psi = 90^\circ$ angle. The critical Rayleigh number for angles $\psi < 90^\circ$ is zero. This means that the circulation of the fluid around the loop begins after the start up of the heating (Fig. 6).

3. Two-phase thermosyphon loop with heated from lower horizontal and vertical parts and cooled from upper horizontal and vertical parts

The variant of the two-phase closed thermosyphon loop consists of two heaters and two coolers connected by channels. A schematic diagram of a one-dimensional model of the thermosyphon loop is shown in Fig. 7. The thermosyphon loop is heated from lower horizontal section ($s_0 \leq s \leq s_1$) and lower vertical section ($s_3 \leq s \leq s_4$) by a constant heat flux: \dot{q}_{H1} and \dot{q}_{H2} , respectively and cooled in the upper horizontal section ($s_6 \leq s \leq s_7$) and upper vertical section ($s_9 \leq s \leq s_{10}$) by a constant heat flux: \dot{q}_{C1} and \dot{q}_{C2} , respectively.

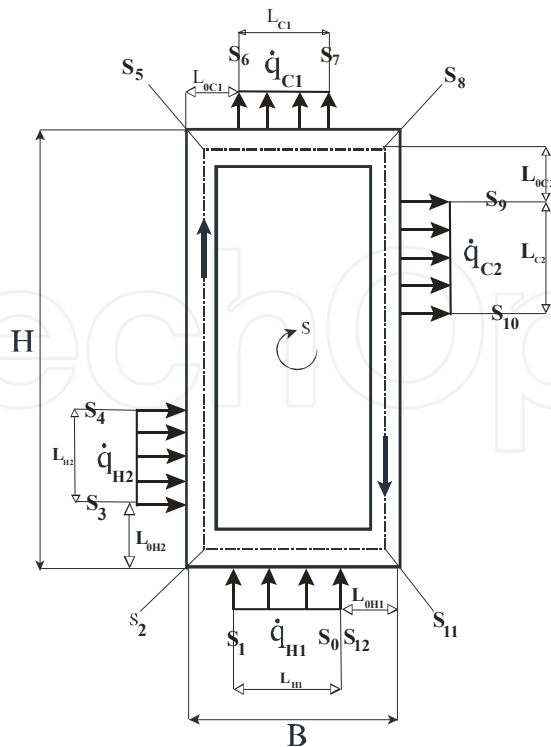


Fig. 7. A schematic diagram of a one-dimensional model of the thermosyphon loop (2H2C)

The constant heat fluxes \dot{q}_{H1} , \dot{q}_{H2} and \dot{q}_{C1} , \dot{q}_{C2} are applied in the cross-section area per heated and cooled length: L_{H1} , L_{H2} and L_{C1} , L_{C2} , respectively. The heated and cooled parts of the thermosyphon loop are connected by perfectly insulated channels ($s_1 \leq s \leq s_3$), ($s_4 \leq s \leq s_6$), ($s_7 \leq s \leq s_9$), ($s_{10} \leq s \leq s_{12}$).

The coordinate s along the loop and the characteristic geometrical points on the loop are marked with s_j , as shown in Fig. 7. The total length of the loop is denoted by L , the cross-section area of the channel by A and the wetted perimeter by U . Thermal properties of fluid: ρ - density, c_p - heat capacity of constant pressure, λ - thermal conductivity.

The following additional assumptions are made in this study:

1. heat exchangers in the thermosyphon loop can be equipped by minichannels,
2. two-phase fluid can be selected as the working fluid,
3. friction coefficient is constant in each region of the loop, separate two-phase flow model can be used in calculations for the frictional pressure loss in the heated, cooled and adiabatic two-phase sections; the two-phase friction factor multiplier $R = \phi_{L0}^2$ is used; the density in the gravity term can be approximated as follows: $\rho = \alpha \cdot \rho_v + (1 - \alpha) \cdot \rho_L$, where α is a void fraction,
4. quality of vapour in the two-phase regions is assumed to be a linear function of the coordinate around the loop,
5. effect of superheating and subcooling are neglected.

In order to eliminate the pressure gradient and the acceleration term, the momentum

equation in Eq. (2) is integrated around the loop $\oint \left(\frac{\partial p}{\partial s} \right) ds = 0$.

After integrating the gravitational term in the momentum equation (2) around the loop, we obtain

$$\oint \{ \epsilon \cdot g \cdot \rho \} ds = g \cdot (\rho_V - \rho_L) \cdot \left\{ (s_3 - s_2) \cdot \bar{\alpha}_{(s_1; s_3)} + (s_4 - s_3) \cdot \bar{\alpha}_{(s_3; s_4)} + (s_5 - s_4) \cdot \bar{\alpha}_{(s_4; s_6)} + \right. \\ \left. - (s_9 - s_8) \cdot \bar{\alpha}_{(s_7; s_9)} - (s_{10} - s_9) \cdot \bar{\alpha}_{(s_9; s_{10})} \right\} = 0 ; \quad (11)$$

where $\bar{\alpha}_{(s_p; s_K)} = \frac{1}{(s_K - s_p)} \cdot \int_{s_p}^{s_K} \alpha_{(s_p; s_K)}(s) ds$.

Due to the friction of fluid, the pressure losses in two-phase regions can be calculated as

$$\frac{U}{A} \cdot \tau_w = \left(\frac{-dp}{ds} \right)_{2p} = R \cdot \left(\frac{-dp}{ds} \right)_{L0} \quad (12)$$

where: $\left(\frac{dp}{ds} \right)_{L0} = \frac{2 \cdot f_{L0}^{Chur} \cdot (\dot{G})^2}{D \cdot \rho_L}$ is the liquid only frictional pressure gradient calculated for the total liquid mass velocity, $\dot{G} = \rho \cdot w$, f_{L0}^{Chur} is friction factor of the fluid (Churchill, 1977). After integrating the friction term in Eq. (2) around the loop, the solution is obtained as follows

$$\oint \left(\frac{U}{A} \cdot \tau_w \right) ds = \left(\frac{dp}{ds} \right)_{L0} \cdot \left\{ (s_1 - s_0) \cdot \bar{R}_{(s_0; s_1)} + (s_3 - s_1) \cdot \bar{R}_{(s_1; s_3)} + (s_4 - s_3) \cdot \bar{R}_{(s_3; s_4)} + \right. \\ \left. + (s_6 - s_4) \cdot \bar{R}_{(s_4; s_6)} + (s_7 - s_6) \cdot \bar{R}_{(s_6; s_7)} + (s_9 - s_7) \cdot \bar{R}_{(s_7; s_9)} + (s_{10} - s_9) \cdot \bar{R}_{(s_9; s_{10})} + (s_{12} - s_{10}) \right\} ; \quad (13)$$

3.1 Minichannels. Distribution of the mass flux

The following correlations have been used in calculation of the thermosyphon loop with minichannels (Table 1): the El-Hajal correlation for void fraction (El-Hajal et al., 2003), the Zhang-Webb correlation for the friction pressure drop of two-phase flow in adiabatic region (Zhang & Webb, 2001), the Tran correlation for the friction pressure drop of two-phase flow in diabatic region (Tran et al. 2000).

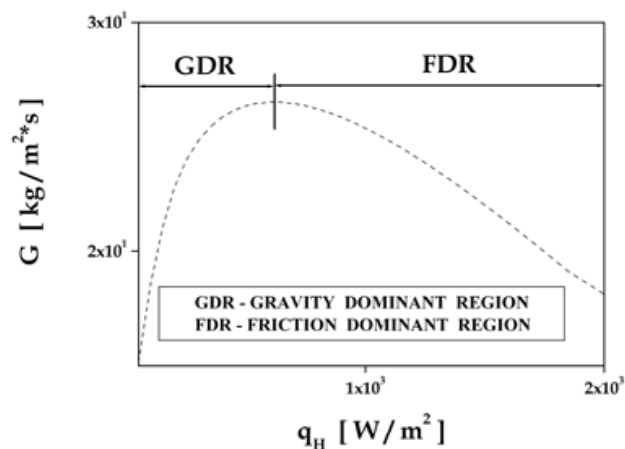


Fig. 8. Minichannels. Mass flux \dot{G} as a function of \dot{q}_H for the steady state (2H2C), ($L=0.2$ [m], $D=0.002$ [m], $H=0.07$ [m], $B=0.03$ [m], $L_{H1}=L_{H2}=L_{C1}=L_{C2}=0.02$ [m], $L_{H1P}=L_{H2P}=L_{C1P}=L_{C2P}=0.005$ [m])

Researcher	Correlation
El-Hajal et al., (2003)	$\alpha_{\text{HAJAL}} = \frac{\alpha_{\text{HOM}} - \alpha_{\text{STEINER}}}{\ln\left(\frac{\alpha_{\text{HOM}}}{\alpha_{\text{STEINER}}}\right)}; \alpha_{\text{HOM}} = \frac{1}{1 + \frac{1-x}{x} \cdot \left(\frac{\rho_v}{\rho_L}\right)};$ $\alpha_{\text{STEINER}} = \left(\frac{x}{\rho_v}\right) \times \left\{ \left[1 + 0.12 \cdot (1-x) \right] \cdot \left[\frac{x}{\rho_v} + \frac{1-x}{\rho_L} \right] + \frac{1.18 \cdot (1-x) \cdot \left[g \cdot \sigma \cdot (\rho_L - \rho_v) \right]^{0.25}}{\dot{G} \cdot (\rho_L)^{0.5}} \right\}^{(-1)};$ (14)
Zhang & Webb, (2001)	$\left(\frac{dp}{dl}\right)_{2p}^{Z-W} = \Phi_{L0}^2 \cdot \left(\frac{dp}{dz}\right)_{L0};$ $\Phi_{L0}^2 = (1-x)^2 + 2.87 \cdot (x)^2 \cdot \left(\frac{P}{P_{\text{CRIT}}}\right)^{(-1)} + 1.68 \cdot (1-x)^{0.25} \cdot \left(\frac{P}{P_{\text{CRIT}}}\right)^{(-1.64)};$ (15)
Tran et al., (2000)	$\left(\frac{dp}{dl}\right)_{2p}^{\text{TRAN}} = \Phi_{L0}^2 \cdot \left(\frac{dp}{dz}\right)_{L0};$ $\Phi_{L0}^2 = 1 + (4.3 \cdot Y^2 - 1) \cdot \left[N_{\text{CONF}} \cdot (x)^{0.875} \cdot (1-x)^{0.875} + (x)^{1.75} \right];$ $N_{\text{CONF}} = \frac{\left[\frac{\sigma}{g \cdot (\rho_L - \rho_v)} \right]^{0.5}}{D}; Y = \sqrt{\left(\frac{dp}{dz}\right)_{v0} / \left(\frac{dp}{dz}\right)_{L0}};$ (16)

Table 1. Minichannels. Correlation for the void fraction and the friction pressure drop of two-phase flow

The mass flux distributions \dot{G} versus heat flux \dot{q}_H for the steady-state conditions and for the minichannels case, is shown in Fig. 8. Two flow regimes can be clearly identified in Fig. 8, namely GDR - gravity dominant regime and FDR - friction dominant regime (Vijayan et al., 2005). Calculations were carried out using the separate model of two-phase flow. The working fluid was distilled water.

3.2 Minichannels. The distributions of heat transfer coefficient in flow boiling

The heat transfer coefficient in flow boiling was calculated for minichannels using the Mikielewicz formula (Mikielewicz et al., 2007) and also calculated using the modified Saitoh formula (Saitoh et al., 2007). The heat transfer coefficient in flow boiling for minichannels h_{TPB} versus heat flux \dot{q}_{H1} in the first evaporator is presented in Fig. 9.

Researcher	Correlation
Mikielewicz et al., (2007)	$\frac{h_{TPB}^{JM}}{h_{REF}} = \sqrt{\left(R_{M-S}\right)^n + \frac{1}{1+P} \cdot \left(\frac{h_{PB}}{h_{REF}}\right)^2} ;$ $R_{M-S} = \left[1 + 2 \cdot \left(\frac{1}{f_1} - 1\right) \cdot x \cdot (N_{CONF})^{(-1)}\right] \cdot (1-x)^{\frac{1}{3}} + x^3 \cdot \frac{1}{f_{1z}} ;$ $LAM \Rightarrow n = 2 ; \alpha_{REF}^{LAM} = 4.36 \cdot \left(\frac{\lambda_L}{D}\right) ; f_1^{LAM} = \left(\frac{\mu_L}{\mu_V}\right) \cdot \left(\frac{\rho_V}{\rho_L}\right) ; f_{1z}^{LAM} = \left(\frac{\lambda_L}{\lambda_V}\right) ;$ $TUR \Rightarrow n = 0.76 ; h_{REF} = 0.023 \cdot \frac{\lambda_L}{D} \cdot (Re_{L0})^{0.8} \cdot (Pr_L)^{\frac{1}{3}} ; \tag{17}$ $f_1^{TUR} = \left(\frac{\mu_L}{\mu_V}\right)^{0.25} \cdot \left(\frac{\rho_V}{\rho_L}\right) ; f_{1z}^{TUR} = \left(\frac{\mu_V}{\mu_L}\right)^{\frac{7}{15}} \cdot \left(\frac{c_{pL}}{c_{pV}}\right)^{\frac{1}{3}} \cdot \left(\frac{\lambda_L}{\lambda_V}\right)^{\frac{3}{2}} ;$ $P = 2.53 \times 10^{(-3)} \cdot (Re_{L0})^{1.17} \cdot (Bo)^{0.6} \cdot (R_{M-S} - 1)^{(-0.65)} ; (Bo) = \frac{\dot{q}}{\dot{G} \cdot r} ; (Re_{L0}) = \frac{\dot{G} \cdot d}{\mu_L} ;$ $h_{PB} = 55 \cdot \dot{q}^{0.67} \cdot M^{(-0.5)} \cdot \left(\frac{P_n}{P_{CRIT}}\right)^{0.12} \cdot \left[-\log_{10}\left(\frac{P_n}{P_{CRIT}}\right)\right]^{(-0.55)} ;$
Saitoh et al., (2007)	$h_{TPB}^{SAITOH} = E \cdot h_{REF} + S \cdot h_{POOL} ;$ $h_{POOL} = 207 \cdot \left(\frac{\lambda_L}{d_b}\right) \cdot \left(\frac{q \cdot d_b}{\lambda_L \cdot T_{SAT}}\right)^{0.745} \cdot \left(\frac{\rho_G}{\rho_L}\right)^{0.581} \cdot (Pr_L)^{0.533} ;$ $h_{REF} = \begin{cases} (Nu)_{LAM} \cdot \left(\frac{\lambda_L}{D}\right) ; & LAM \\ 0.023 \cdot (Re_L)^{\frac{4}{5}} \cdot (Pr_L)^{0.4} \cdot \left(\frac{\lambda_L}{D}\right) ; & TUR \end{cases}$ $E = 1 + \frac{\left(\frac{1}{X}\right)^{1.05}}{1 + (We_G)^{(-0.4)}} ; (Re_G) = \frac{\dot{G}_G \cdot D}{\mu_G} ; (Re_L) = \frac{\dot{G}_L \cdot D}{\mu_L} ; \tag{18}$ $S = \frac{1}{1 + 0.4 \cdot \left[\left(10^{(-4)}\right) \cdot (Re_{TP})\right]^{1.4}} ; d_b = 0.51 \cdot \left(\frac{2 \cdot \sigma}{g \cdot (\rho_L - \rho_G)}\right)^{0.5} ;$ $(We_G) = \frac{\dot{G}_G \cdot D}{\sigma \cdot \rho_G} ; (Re_{TP}) = (Re_L) \cdot (F)^{1.25} ; \dot{G}_G = \dot{G} \cdot x ; \dot{G}_L = \dot{G} \cdot (1-x) ;$ $X = \left(\frac{1-x}{x}\right)^{0.9} \cdot \left(\frac{\rho_G}{\rho_L}\right)^{0.5} \cdot \left(\frac{\mu_L}{\mu_G}\right)^{0.1} \text{ for } \begin{cases} (Re_L) > 1000 \\ (Re_G) > 1000 \end{cases} ;$ $C_G = 0.046 ; C_L = 16 ;$ $X = \left(\frac{C_L}{C_G}\right)^{0.5} \times (Re_G)^{(-0.4)} \times \left(\frac{G_L}{G_G}\right)^{0.5} \cdot \left(\frac{\rho_G}{\rho_L}\right)^{0.5} \cdot \left(\frac{\mu_L}{\mu_G}\right)^{0.5} \text{ for } \begin{cases} (Re_L) < 1000 \\ (Re_G) > 1000 \end{cases} ;$

Table 2. Minichannels. Correlation for the heat transfer coefficient in flow boiling

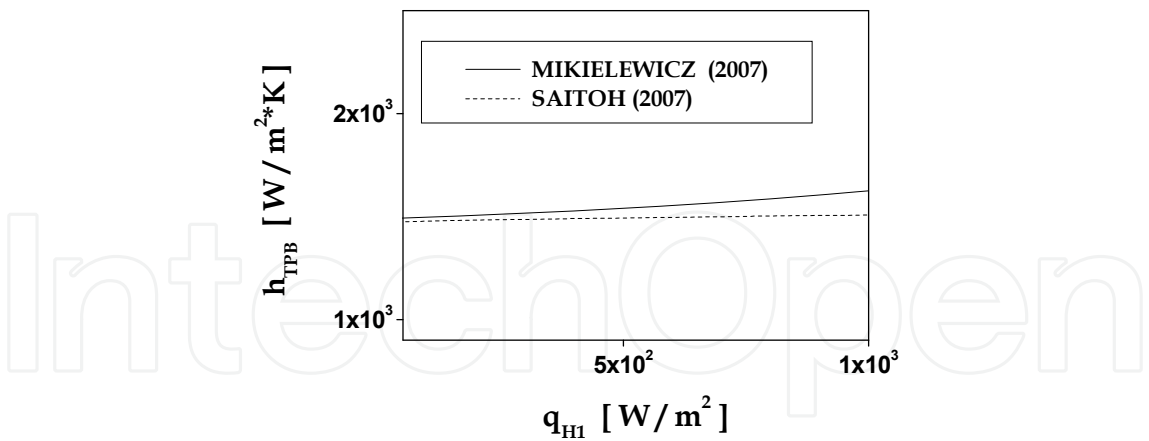


Fig. 9. Minichannels. Heat transfer coefficient in flow boiling h_{TPB} as a function of \dot{q}_{H1} in the first evaporator. ($L=0.2$ [m], $D=0.002$ [m], $H=0.07$ [m], $B=0.03$ [m], $L_{H1}=L_{H2}=L_{C1}=L_{C2}=0.02$ [m], $L_{H1P}=L_{H2P}=L_{C1P}=L_{C2P}=0.005$ [m])

3.3 Minichannels. The heat transfer coefficient in condensation

The condensation heat transfer coefficient for minichannels was calculated using the Mikielewicz formula Eq. (17). The term which describes nucleation process in this formula was neglected. The heat transfer coefficient for condensation in minichannels was also calculated using the modified Tang formula (Tang et al., 2000).

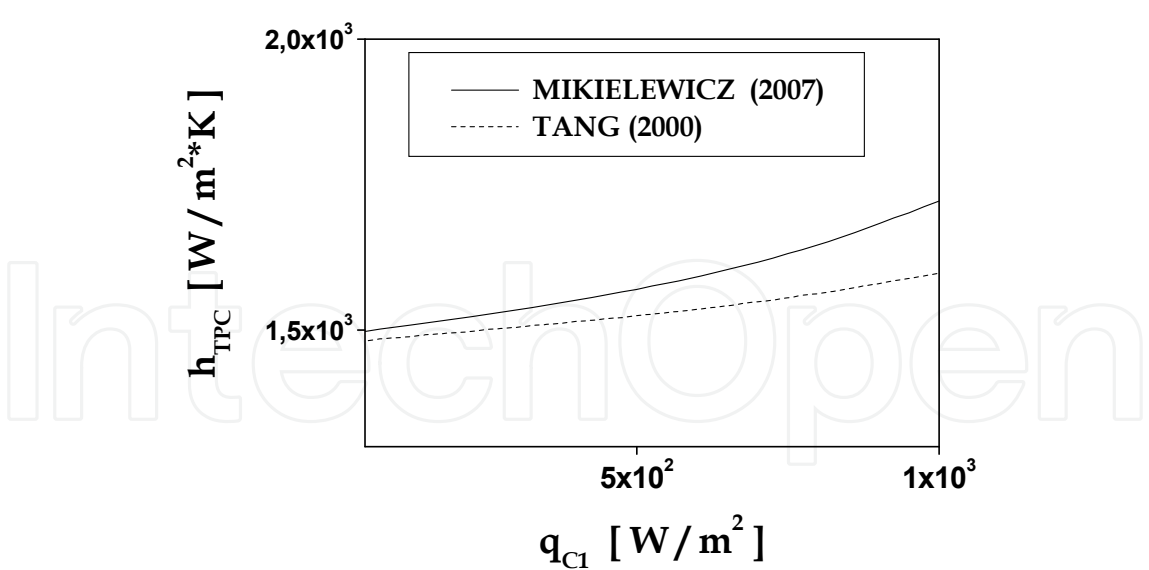


Fig. 10. Minichannels. Heat transfer coefficient h_{TPC} as a function of \dot{q}_{C1} in the first condenser. ($L=0.2$ [m], $D=0.002$ [m], $H=0.07$ [m], $B=0.03$ [m], $L_{H1}=L_{H2}=L_{C1}=L_{C2}=0.02$ [m], $L_{H1P}=L_{H2P}=L_{C1P}=L_{C2P}=0.005$ [m])

The condensation heat transfer coefficient for minichannels h_{TPC} versus heat flux \dot{q}_{C1} in the first condenser is presented in Fig. 10.

Researcher	Correlation
Mikielewicz et al., (2007)	$\frac{h_{TPB}^{JM}}{h_{REF}} = \sqrt{(R_{M-S})^n} \quad ; \quad (19)$
Tang et al., (2000)	$h_{TPC}^{TANG} = (Nu) \cdot \left(\frac{\lambda_L}{D} \right) \cdot \left[1 + 4.863 \cdot \frac{\left((-x) \cdot \left[\ln \left(\frac{P_{SAT}}{P_{CRIT}} \right) \right] \right)^{0.836}}{(1-x)} \right] \quad ; \quad (20)$

Table 3. Minichannels. Correlation for the condensation heat transfer coefficient

3.4 The effect of geometrical and thermal parameters on the mass flux distributions

The effect of the internal diameter tube D on the mass flux for the steady-state conditions is presented in Fig. 11. The mass flux rapidly increases with increasing internal diameter tube D . The GDR (Gravity Dominant Region) decreases with decreasing internal diameter tube D .

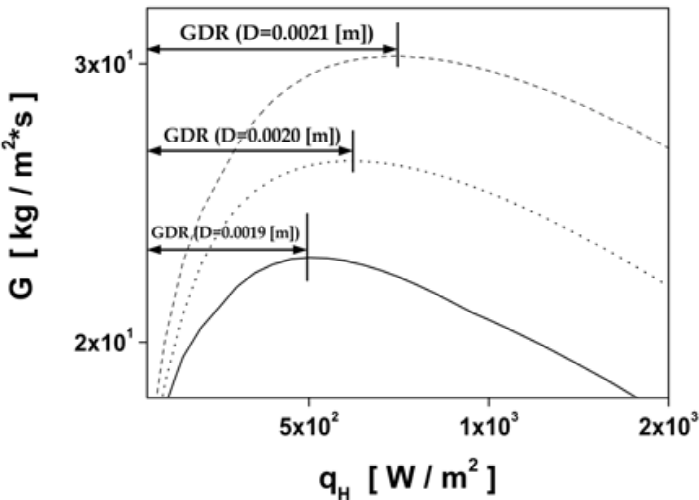


Fig. 11. Mass flux \dot{G} as a function of \dot{q}_H with internal diameter tube D as the parameter (2H2C). ($L=0.2$ [m], $H=0.07$ [m], $B=0.03$ [m], $L_{H1}=L_{H2}=L_{C1}=L_{C2}=0.02$ [m], $L_{H1P}=L_{H2P}=L_{C1P}=L_{C2P}=0.005$ [m])

The effect of length of the heated section L_{H2} on the mass flux is demonstrated in Fig. 13. If the length of horizontal section B is constant, the mass flux increases with increasing length of vertical section H due to the increasing gravitational pressure drop. The increase in length of the vertical section H induces an increase in both the gravitational and frictional pressure drop. However, the gravitational pressure drop grows more in comparison to frictional pressure drop.

The effect of length of the heated section L_{H2} on the mass flux is demonstrated in Fig. 12. The mass flux increases with increasing length of the heated section L_{H2} in gravity dominant region (GDR) but in friction dominant region (FDR) the mass flux decreases with increasing length of the heated section L_{H2} .

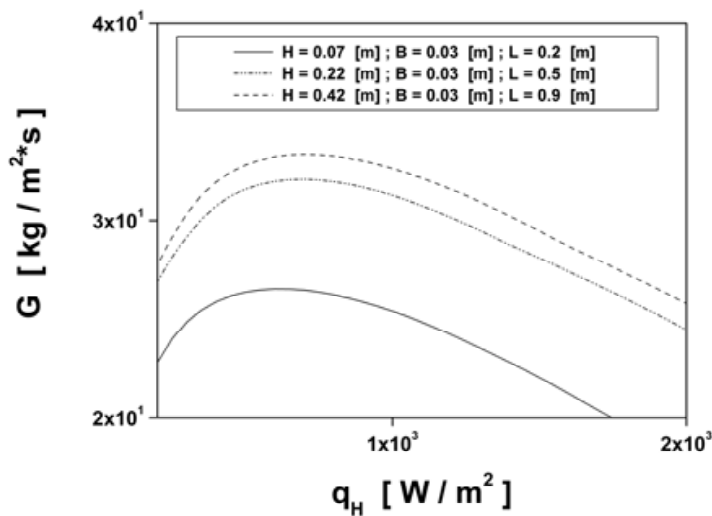


Fig. 12. Mass flux \dot{G} as a function of \dot{q}_H with parameter H (2H2C).
($D=0.002$ [m], $B=0.03$ [m], $L_{H1}=L_{H2}=L_{C1}=L_{C2}=0.02$ [m], $L_{H1P}=L_{H2P}=L_{C1P}=L_{C2P}=0.005$ [m])

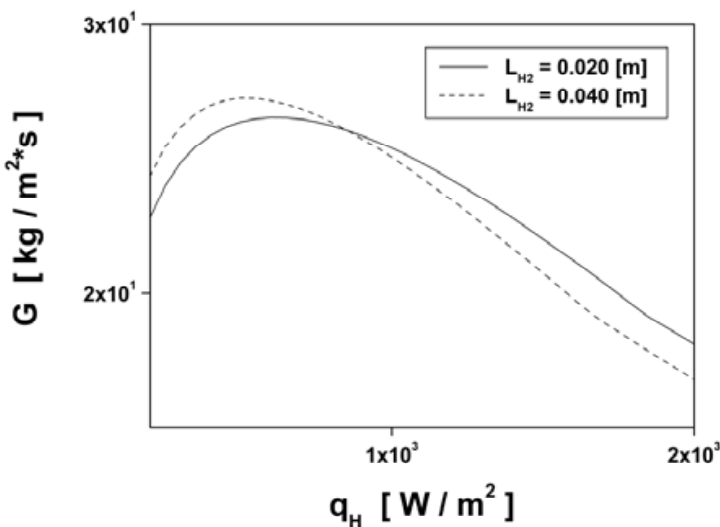


Fig. 13. Mass flux \dot{G} as a function of \dot{q}_H with parameter L_{H2} (2H2C).
($L=0.2$ [m], $D=0.002$ [m], $H=0.07$ [m], $B=0.03$ [m], $L_{H1}=L_{C1}=L_{C2}=0.02$ [m],
 $L_{H1P}=L_{H2P}=L_{C1P}=L_{C2P}=0.005$ [m])

The effect of length of the preheated section L_{H2P} on the mass flux is shown in Fig. 14. The mass flux increases with decreasing length of the preheated section L_{H2P} , in gravity dominant region (GDR) due to the increasing of the gravitational driving force.

The effect of length of the cooled section L_{C2} on the mass flux is given in Fig. 15. The mass flux decreases with increasing length of cooled section L_{C2} due to the increasing length of two-phase friction section $\langle s_9; s_{10} \rangle$ and the increasing frictional pressure drop.

The effect of length of the precooled section L_{C2P} on the mass flux is presented in Fig. 16. The mass flux increases with decreasing length of the precooled section L_{C2P} due to the increasing gravitational driving force.

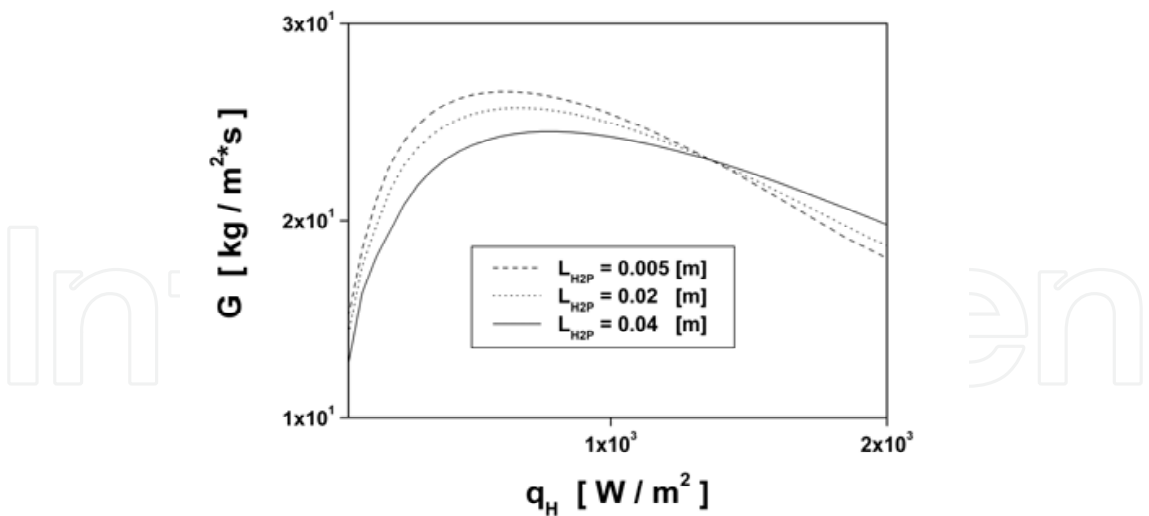


Fig. 14. Mass flux \dot{G} as a function of \dot{q}_H with parameter L_{H2P} (2H2C).
($L=0.2$ [m], $D=0.002$ [m], $H=0.07$ [m], $B=0.03$ [m], $L_{H1}=L_{H2}=L_{C1}=L_{C2}=0.02$ [m],
 $L_{H1P}=L_{C1P}=L_{C2P}=0.005$ [m])

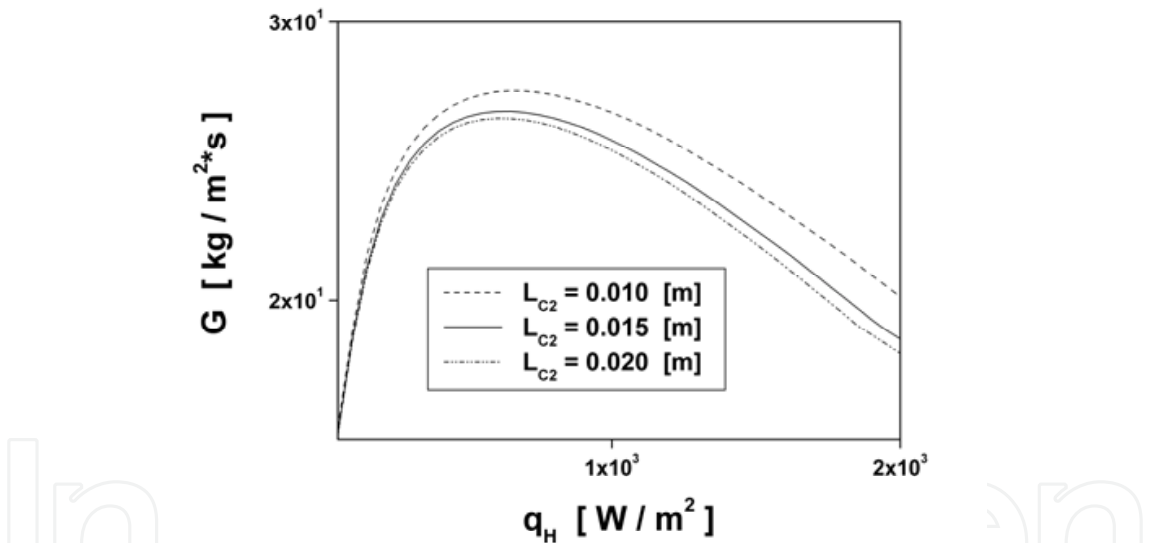


Fig. 15. Mass flux \dot{G} as a function of \dot{q}_H with L_{C2} as a parameter (2H2C).
($L=0.2$ [m], $D=0.002$ [m], $H=0.07$ [m], $B=0.03$ [m], $L_{H1}=L_{H2}=L_{C1}=0.02$ [m],
 $L_{H1P}=L_{H2P}=L_{C1P}=L_{C2P}=0.005$ [m])

The effect of width B of the loop on the mass flux is given in Fig. 17. If the height H of the loop is constant the mass flux decreases with the increasing width B of the loop, due to the increasing frictional pressure drop. No change of the gravitational pressure drop is observed because the height H of the loop is constant.

The effect of heat flux ratio $\dot{q}_{H1}/\dot{q}_{H2}$ on the mass flux \dot{G} versus \dot{q}_H for the steady-state conditions is presented in Fig. 18. The mass flux increases with increasing of heat flux ratio $\dot{q}_{H1}/\dot{q}_{H2}$.

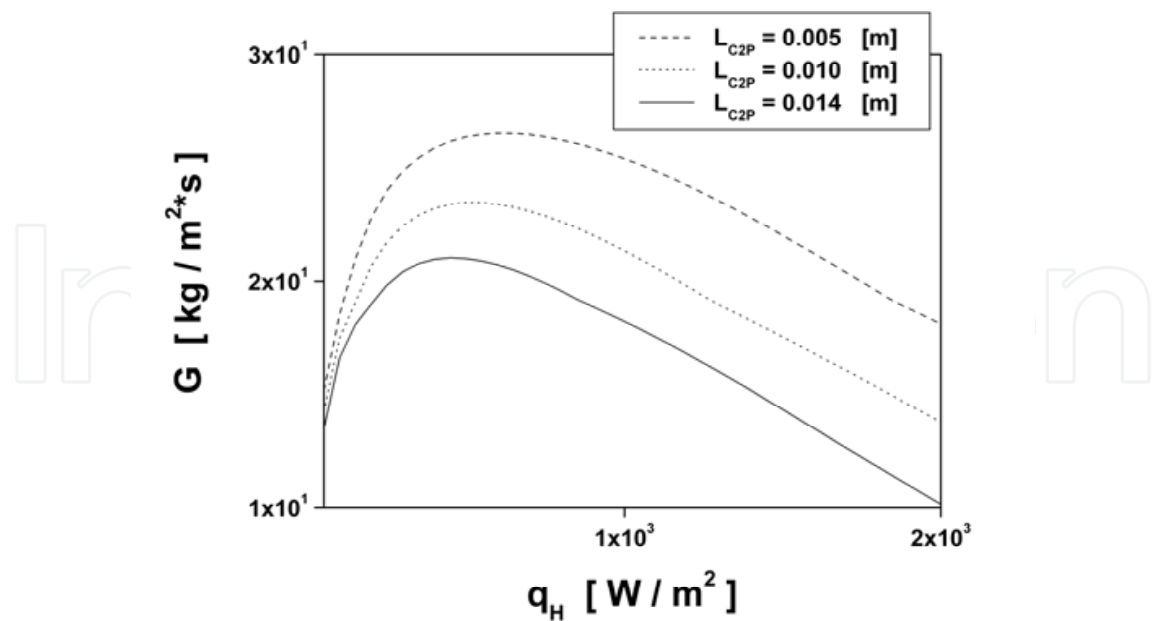


Fig. 16. Mass flux \dot{G} as a function of \dot{q}_H with L_{C2P} as a parameter (2H2C).
($L=0.2$ [m], $D=0.002$ [m], $H=0.07$ [m], $B=0.03$ [m], $L_{H1}=L_{H2}=L_{C1}=L_{C2}=0.02$ [m],
 $L_{H1P}=L_{H2P}=L_{C1P}=0.005$ [m])

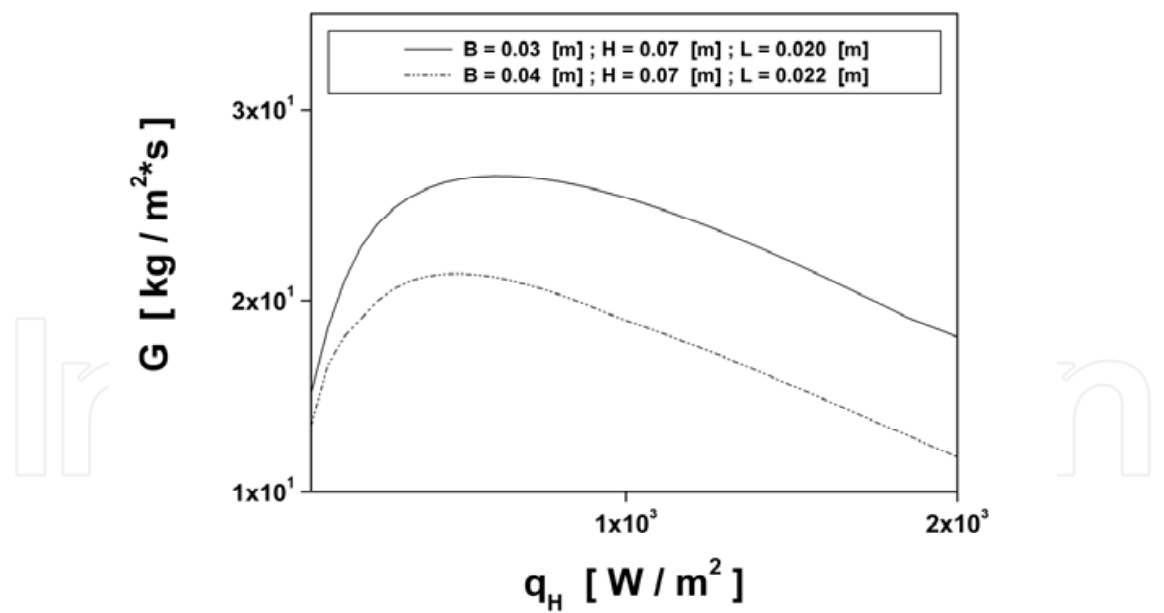


Fig. 17. Mass flux \dot{G} as a function of \dot{q}_H with parameter B (width of the loop) (2H2C).
($D=0.002$ [m], $H=0.07$ [m], $L_{H1}=L_{H2}=L_{C1}=L_{C2}=0.02$ [m], $L_{H1P}=L_{H2P}=L_{C1P}=L_{C2P}=0.005$ [m])

The effect of heat flux ratio $\dot{q}_{C1}/\dot{q}_{C2}$ on the mass flux \dot{G} versus \dot{q}_H for the steady-state conditions is presented in Fig. 19. The mass flux increases with increasing of heat flux ratio $\dot{q}_{C1}/\dot{q}_{C2}$.

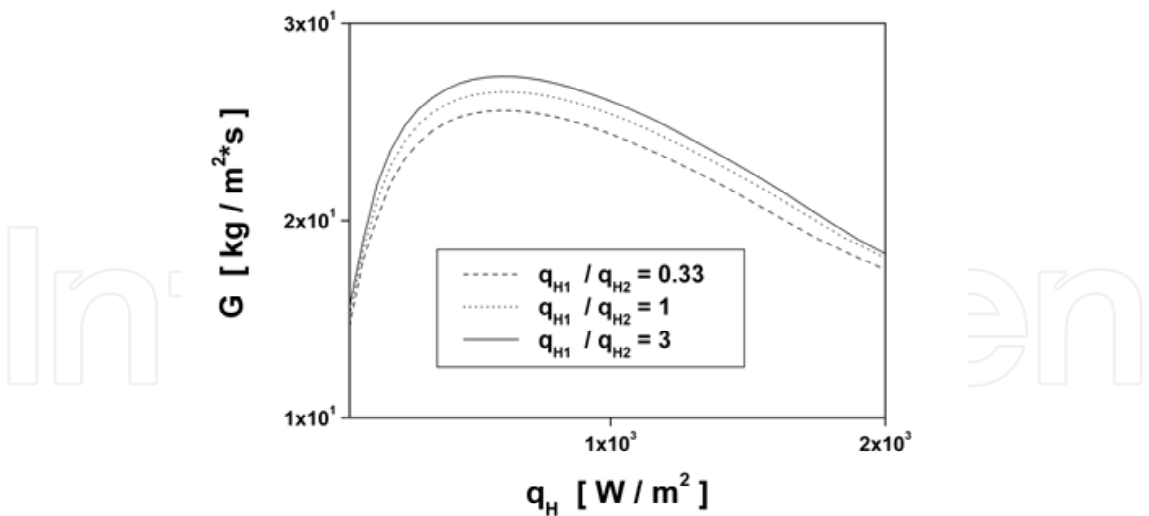


Fig. 18. Mass flux \dot{G} as a function of \dot{q}_H with parameter $\dot{q}_{H1}/\dot{q}_{H2}$ (2H2C).
($L=0.2$ [m], $D=0.002$ [m], $H=0.07$ [m], $B=0.03$ [m], $L_{H1}=L_{H2}=L_{C1}=L_{C2}=0.02$ [m],
 $L_{H1P}=L_{H2P}=L_{C1P}=L_{C2P}=0.005$ [m])

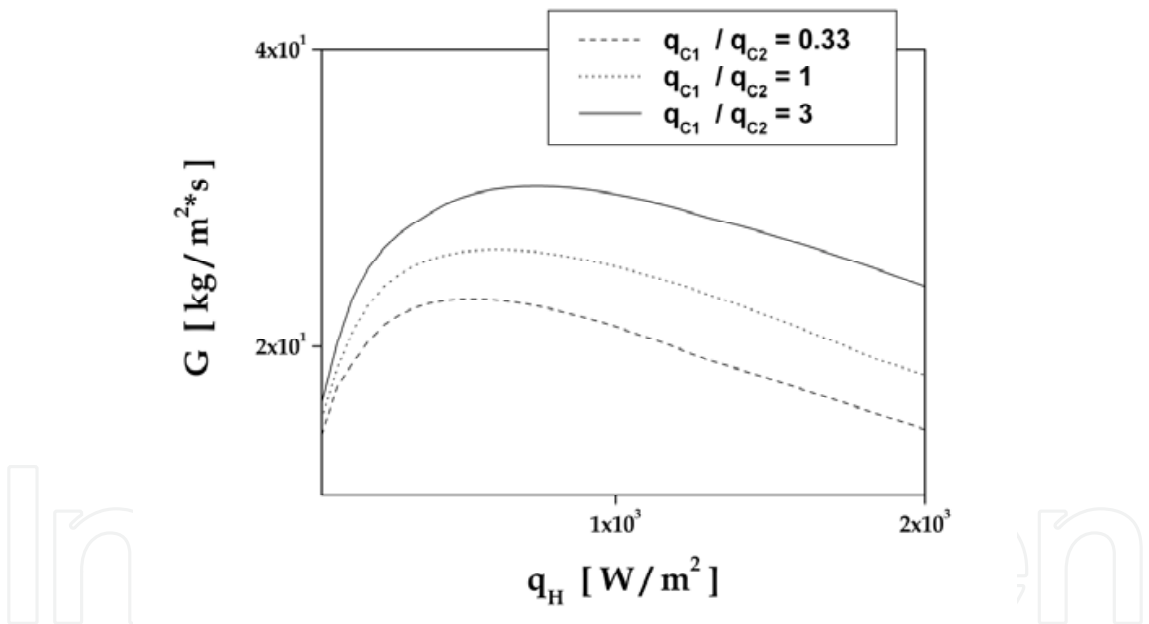


Fig. 19. Mass flux \dot{G} as a function of \dot{q}_H with parameter $\dot{q}_{C1}/\dot{q}_{C2}$ (2H2C).
($L=0.2$ [m], $D=0.002$ [m], $H=0.07$ [m], $B=0.03$ [m], $L_{H1}=L_{H2}=L_{C1}=L_{C2}=0.02$ [m],
 $L_{H1P}=L_{H2P}=L_{C1P}=L_{C2P}=0.005$ [m])

4. Two-phase thermosyphon loop with minichannels and minipump heated from lower horizontal section and cooled from upper vertical section

A schematic diagram of thermosyphon loop heated from horizontal side and cooled from vertical side with minipump is shown in Fig. 20 . The minipump can be used if the mass flux is not high enough to transport heat from evaporator to condenser. Therefore, the

minipump promotes natural circulation. In the equation of motion of the thermosyphon loop with natural circulation, the pressure term of integration around the loop is zero

$\oint \left(\frac{dp}{ds} \right) ds = 0$. For the thermosyphon loop with minipump the pressure term is

$$\oint \left(\frac{dp}{ds} \right) ds = \Delta p_{\text{PUMP}} = \rho_L \cdot g \cdot H_{\text{PUMP}} ; H_{\text{PUMP}} = H_{\text{MAX}} \cdot \left[1 - \left(\frac{\dot{V}}{\dot{V}_{\text{MAX}}} \right)^2 \right], \text{ with } H_{\text{MAX}}, \dot{V}_{\text{MAX}} \text{ from}$$

minipump curve (\dot{V} - volumetric flow rate).

A schematic diagram of a one-dimensional model of the thermosyphon loop with minipump is shown in Fig. 20.

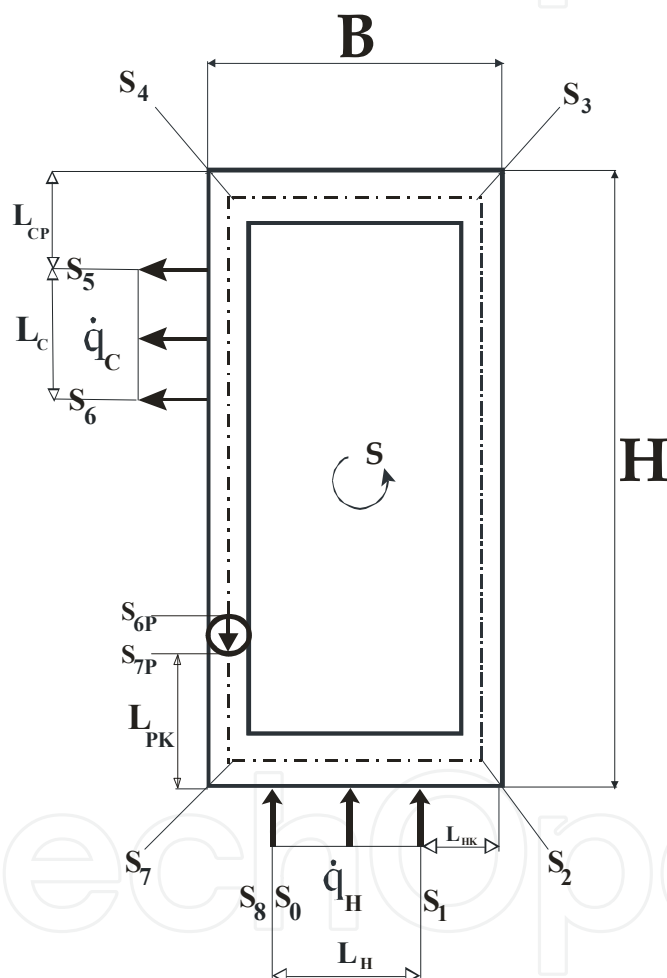


Fig. 20. A schematic diagram of a one-dimensional model of the thermosyphon loop with minipump (HHCV+P)

The mass flux distributions \dot{G} versus heat flux \dot{q}_H for the steady-state conditions and for minichannels, is shown in Fig. 21. Calculations were carried out using the separate model of two-phase flow. The following correlations have been used in the calculation: the El-Hajal correlation (Eq. 21) for void fraction (El-Hajal et al., 2003), the Zhang-Webb correlation (Eq. 22) for the friction pressure drop of two-phase flow in adiabatic region (Zhang & Webb, 2001), the Tran correlation (Eq. 23) for the friction pressure drop of two-phase flow in

diabatic region (Tran et al. 2000). The working fluid was distilled water. A miniature pump curve from (Blanchard et. al., 2004) was included in the calculation. The Fig. 21 shows the mass flux \dot{G} decreases with increasing heat flux \dot{q}_H for minichannels with minipump (HHCV+P) for the steady-state condition.

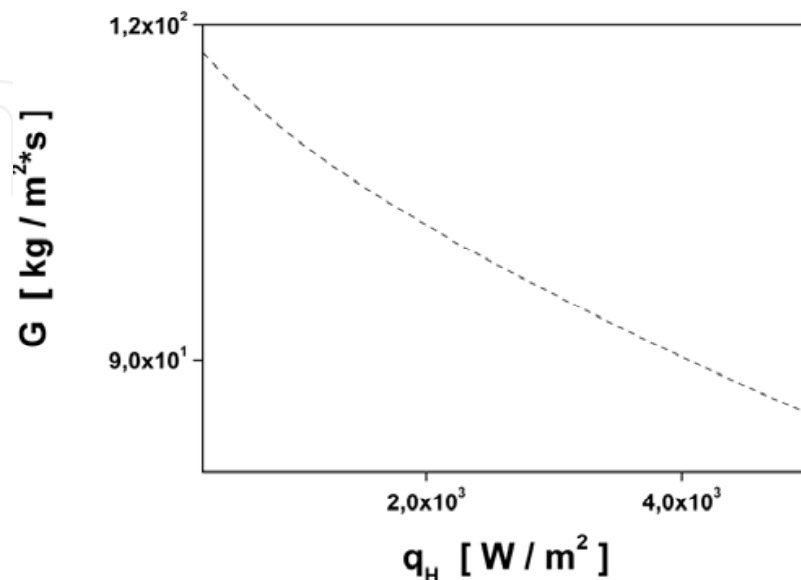


Fig. 21. Distributions of the mass flux \dot{G} versus heat flux \dot{q}_H , for the steady-state conditions for minichannels with minipump (HHCV+P). ($L=0.2$ [m], $D=0.002$ [m], $H=0.09$ [m], $B=0.01$ [m], $L_H=L_C=0.008$ [m], $L_{HP}=L_{CP}=0.0001$ [m], $L_{PK}=0.0001$ [m])

5. Conclusions

The presented new variants (HHVCHV, 2H2C, HHCV+P) and the previous variants (HHCH, HVCV, HHCV) described in the chapter (Bieliński & Mikielewicz, 2011) can be analyzed using the conservation equations of mass, momentum and energy based on the generalized model of the thermosyphon loop. This study shows that the new effective numerical method proposed for solving the problem of the onset of motion in a fluid from the rest can be applied for the following variants: (HHVCHV+ $\psi 90^\circ$) and (HHCH).

The results of this study indicate that the properties of the variants associated with the generalized model of thermosyphon loop depend strongly on their specific technical conditions. For this reasons, the theoretical analysis of the presented variants can be applied, for example, to support the development of an alternative cooling technology for electronic systems. The progress in electronic equipment is due to the increased power levels and miniaturization of devices. The traditional cooling techniques are not able to cool effectively at high heat fluxes. The application of mini-loops can be successful by employing complex geometries, in order to maximize the heat transferred by the systems under condition of single- and two phase flows.

The obtained results show that the one-dimensional two-phase separate flow model can be used to describe heat transfer and fluid flow in the thermosyphon loop for minichannels. The evaluation of the thermosyphon loop with minichannels can be done in calculations using correlations such as the El-Hajal correlation (El-Hajal et al., 2003) for void fraction, the

Zhang-Webb correlation (Zhang & Webb, 2001) for the friction pressure drop of two-phase flow in adiabatic region, the Tran correlation (Tran et al., 2000) for the friction pressure drop of two-phase flow in diabatic region and the Mikielwicz correlation (Mikielwicz et al., 2007) for the heat transfer coefficient in evaporator and condenser.

Two flow regimes such as GDR- gravity dominant regime and FDR – friction dominant regime can be clearly identified (Fig. 8). The distribution of the mass flux against the heat flux approaches a maximum and then slowly decreases for minichannels. The effect of geometrical and thermal parameters on the mass flux distributions was obtained numerically for the steady-state conditions as presented in Figs. 11-19. The mass flux strongly increases with the following parameters: (a) increasing of the internal tube diameter, (b) increasing length of the vertical section H, (c) decreasing length of the precooled section L_{C2P} . The mass flux decreases with the parameters, such as (d) increasing length of the cooled section L_{C2} , (e) increasing length of the horizontal section B, (f) decreasing of the heat flux ratio: $\dot{q}_{H1}/\dot{q}_{H2}$ and $\dot{q}_{C1}/\dot{q}_{C2}$. If the mass flow rate is not high enough to circulate the necessary fluid to transport heat from evaporator to condenser, the minipump can be used to promotes natural circulation. For the steady-state condition as is demonstrated in Fig. 21, the mass flux \dot{G} decreases with increasing heat flux \dot{q}_H for minichannels with minipump (HHCV+P).

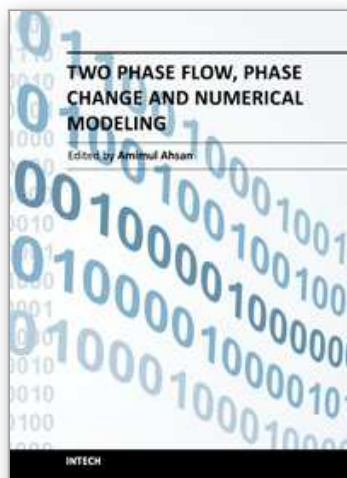
Each variant of thermosyphon loop requires an individual analysis of the effect of geometrical and thermal parameters on the mass flux. Two of the reasons are that the variants include the heated and cooled sections in different places on the loop and may have different quantity of heaters and coolers.

In future the transient analysis should be developed in order to characterize the dynamic behaviour of single- and two phase flow for different combination of boundary conditions. Attempts should be made to verify the presented variants based on numerical calculations for the theoretical model of thermosyphon loops with experimental data.

6. References

- Bieliński, H.; Mikielwicz, J. (1995). Natural Convection of Thermal Diode., *Archives of Thermodynamics*, Vol. 16, No. 3-4.
- Bieliński, H.; Mikielwicz, J. (2001). New solutions of thermal diode with natural laminar circulation., *Archives of Thermodynamics*, Vol. 22, pp. 89-106.
- Bieliński, H.; Mikielwicz J. (2004). The effect of geometrical parameters on the mass flux in a two phase thermosyphon loop heated from one side., *Archives of Thermodynamics*, Vol. 29, No. 1, pp. 59-68.
- Bieliński, H.; Mikielwicz J. (2004). Natural circulation in two-phase thermosyphon loop heated from below., *Archives of Thermodynamics*, Vol. 25, No. 3, pp. 15-26.
- Bieliński, H.; Mikielwicz, J. (2005). A two-phase thermosyphon loop with side heating, *Inżynieria Chemiczna i Procesowa.*, Vol. 26, pp. 339-351 (in Polish).
- Bieliński, H.; Mikielwicz, J. (2010). Energetic analysis of natural circulation in the closed loop thermosyphon with minichannels., *Archiwum Energetyki*, Tom. XL, No 3, pp.3-10,
- Bieliński, H.; Mikielwicz, J. (2010). Computer cooling using a two phase minichannel thermosyphon loop heated from horizontal and vertical sides and cooled from vertical side., *Archives of Thermodynamics*, Vol. 31(2010), No. 4, pp. 51-59.

- Bieliński, H.; Mikielwicz, J. (2010). A Two Phase Thermosyphon Loop With Minichannels Heated From Vertical Side And Cooled From Horizontal Side, *Inżynieria Chemiczna i Procesowa.*, Vol. 31, pp. 535-551 .
- Bieliński, H.; Mikielwicz, J. (2011). Natural Circulation in Single and Two Phase Thermosyphon Loop with Conventional Tubes and Minichannels,. published by InTech (ISBN 978-953-307-550-1) in book *Heat Transfer. Mathematical Modeling, Numerical Methods and Information Technology*, Edited by A. Belmiloudi, pp. 475-496,
- Blanchard, D.B., Ligrani, P.M., Gale, B.K. (2004). Performance and Development of a Miniature Rotary Shaft Pump (RSP)., 2004 ASME International Mechanical Engineering Congress and RD&D Expo, November 13-20, 2004, Anaheim, California USA.
- Chen, K. (1988). Design of Plane-Type Bi-directional Thermal Diode., *ASME J. of Solar Energy Engineering*, Vol. 110.
- Churchill, S.W. (1977). Friction-Factor Equation Spans all Fluid Flow Regimes., *Chem. Eng.*, pp. 91-92.
- El-Hajal, J.; Thome, J.R. & Cavalini A. (2003). Condensation in horizontal tubes, part 1; two-phase flow pattern map., *Int. J. Heat Mass Transfer*, Vol. 46, No. 18, pp. 3349-3363.
- Greif, R. (1988). Natural Circulation Loops., *Journal of Heat Transfer*, Vol. 110, pp. 1243-1257.
- Madejski, J.; Mikielwicz, J. (1971). Liquid Fin - a New Device for Heat Transfer Equipment, *Int. J. Heat Mass Transfer*, Vol. 14, pp. 357-363.
- Mikielwicz, D.; Mikielwicz, J. & Tesmar J. (2007). Improved semi-empirical method for determination of heat transfer coefficient in flow boiling in conventional and small diameter tubes., *Inter. J. Heat Mass Transfe* , Vol. 50, pp. 3949-3956.
- Mikielwicz J. (1995). Modelling of the heat-flow processes., *Polska Akademia Nauk Instytut Maszyn Przepływowych, Seria Ciepłne Maszyny Przepływowe*, Vol. 17, Ossolineum.
- Misale, M.; Garibaldi, P.; Passos, J.C.; Ghisi de Bitencourt, G. (2007). Experiments in a Single-Phase Natural Circulation Mini-Loop., *Experimental Thermal and Fluid Science*, Vol. 31, pp. 1111-1120.
- Ramos, E.; Sen, M. & Trevino, C. (1985). A steady-state analysis for variable area one- and two-phase thermosyphon loops, *Int. J. Heat Mass Transfer*, Vol. 28, No. 9, pp. 1711-1719.
- Saitoh, S.; Daiguji, H. & Hihara, E. (2007). Correlation for Boiling Heat Transfer of R-134a in Horizontal Tubes Including Effect of Tube Diameter., *Int. J. Heat Mass Tr.*, Vol. 50, pp. 5215-5225.
- Tang, L.; Ohadi, M.M. & Johnson, A.T. (2000). Flow condensation in smooth and microfin tubes with HCFC-22, HFC-134a, and HFC-410 refrigerants, Part II: Design equations. *Journal of Enhanced Heat Transfer*, Vol. 7, pp. 311-325.
- Tran, T.N.; Chyu, M.C.; Wambsganss, M.W.; & France D.M. (2000). Two -phase pressure drop of refrigerants during flow boiling in small channels: an experimental investigations and correlation development., *Int. J. Multiphase Flow*, Vol. 26, No. 11, pp. 1739-1754.
- Vijayan, P.K.; Gartia, M.R.; Pilkhwal, D.S.; Rao, G.S.S.P. & Saha D. (2005). Steady State Behaviour Of Single-Phase And Two-Phase Natural Circulation Loops. 2nd RCM on the IAEA CRP ,Corvallis, Oregon State University, USA.
- Zhang, M.; Webb, R.L. (2001). Correlation of two-phase friction for refrigerants in small-diameter tubes. *Experimental Thermal and Fluid Science*, Vol. 25, pp. 131-139.
- Zvirin, Y. (1981). A Review of Natural Circulation Loops in PWR and Other Systems., *Nuclear Engineering Design*, Vol. 67, pp. 203-225.



Two Phase Flow, Phase Change and Numerical Modeling

Edited by Dr. Amimul Ahsan

ISBN 978-953-307-584-6

Hard cover, 584 pages

Publisher InTech

Published online 26, September, 2011

Published in print edition September, 2011

The heat transfer and analysis on laser beam, evaporator coils, shell-and-tube condenser, two phase flow, nanofluids, complex fluids, and on phase change are significant issues in a design of wide range of industrial processes and devices. This book includes 25 advanced and revised contributions, and it covers mainly (1) numerical modeling of heat transfer, (2) two phase flow, (3) nanofluids, and (4) phase change. The first section introduces numerical modeling of heat transfer on particles in binary gas-solid fluidization bed, solidification phenomena, thermal approaches to laser damage, and temperature and velocity distribution. The second section covers density wave instability phenomena, gas and spray-water quenching, spray cooling, wettability effect, liquid film thickness, and thermosyphon loop. The third section includes nanofluids for heat transfer, nanofluids in minichannels, potential and engineering strategies on nanofluids, and heat transfer at nanoscale. The fourth section presents time-dependent melting and deformation processes of phase change material (PCM), thermal energy storage tanks using PCM, phase change in deep CO₂ injector, and thermal storage device of solar hot water system. The advanced idea and information described here will be fruitful for the readers to find a sustainable solution in an industrialized society.

How to reference

In order to correctly reference this scholarly work, feel free to copy and paste the following:

Henryk Bieliński (2011). New Variants to Theoretical Investigations of Thermosyphon Loop, Two Phase Flow, Phase Change and Numerical Modeling, Dr. Amimul Ahsan (Ed.), ISBN: 978-953-307-584-6, InTech, Available from: <http://www.intechopen.com/books/two-phase-flow-phase-change-and-numerical-modeling/new-variants-to-theoretical-investigations-of-thermosyphon-loop>

INTECH
open science | open minds

InTech Europe

University Campus STeP Ri
Slavka Krautzeka 83/A
51000 Rijeka, Croatia
Phone: +385 (51) 770 447
Fax: +385 (51) 686 166
www.intechopen.com

InTech China

Unit 405, Office Block, Hotel Equatorial Shanghai
No.65, Yan An Road (West), Shanghai, 200040, China
中国上海市延安西路65号上海国际贵都大饭店办公楼405单元
Phone: +86-21-62489820
Fax: +86-21-62489821

© 2011 The Author(s). Licensee IntechOpen. This chapter is distributed under the terms of the [Creative Commons Attribution-NonCommercial-ShareAlike-3.0 License](https://creativecommons.org/licenses/by-nc-sa/3.0/), which permits use, distribution and reproduction for non-commercial purposes, provided the original is properly cited and derivative works building on this content are distributed under the same license.

IntechOpen

IntechOpen